

Implementation of Metaheuristic-Optimized Algorithms in Tuning ANFIS for Photovoltaic Power Output Forecasting

Teguh Herlambang

Department of Information Systems, Faculty of Economic Business and Digital Technology, Universitas Nahdlatul Ulama Surabaya, Indonesia
teguh@unusa.ac.id (corresponding author)

Zuraini Othman

Department of Diploma Studies, Fakulti Teknologi Maklumat dan Komunikasi, Universiti Teknikal Malaysia Melaka, Malaysia
zuraini@utem.edu.my

Aniza Othman

Department of Diploma Studies, Fakulti Teknologi Maklumat dan Komunikasi, Universiti Teknikal Malaysia Melaka, Malaysia
aniza@utem.edu.my

Received: 4 March 2026 | Revised: 2 April 2026, 21 April 2026, and 11 May 2026 | Accepted: 27 May 2026

Licensed under a CC-BY 4.0 license | Copyright (c) by the authors | DOI: <https://doi.org/10.48084/etasr.18534>

ABSTRACT

As Indonesia accelerates its transition toward renewable energy utilization, the large-scale deployment of Photovoltaic (PV) systems presents challenges regarding grid stability due to the intermittent nature of solar irradiance. To address this issue, the current study proposes a robust forecasting framework that integrates the Adaptive Neuro-Fuzzy Inference System (ANFIS) with metaheuristic optimization algorithms to accurately predict PV power output. This study focuses on optimizing ANFIS parameters to address the nonlinear complexities inherent in local weather data. Comparative experimental analysis demonstrated that the hybrid approach significantly enhanced prediction performance. The ANFIS-Particle Swarm Optimization (ANFIS-PSO) model outperformed other tested configurations, achieving the highest accuracy with a Root Mean Square Error (RMSE) of 0.68. These findings suggest that the ANFIS-PSO architecture is a highly effective tool for reliable power forecasting, thereby supporting the efficient integration of solar energy into Indonesia's electrical grid.

Keywords-ANFIS; clean energy; electricity; forecasting; photovoltaic

I. INTRODUCTION

The rapid depletion of fossil fuel reserves and the environmental burden of their combustion have intensified the need for a global energy transition. Dependence on coal, oil, and gas is a significant driver of greenhouse gas emissions, air pollution, and the associated health risks, particularly in rapidly urbanizing regions and lower-middle-income countries [1]. Addressing these challenges requires a structural shift toward low-carbon energy systems that can deliver reliable power while reducing environmental and health impacts [2].

Among renewable energy options, Photovoltaics (PVs) contribute significantly to the transition from fossil fuels to clean energy. The annual solar energy incident on Earth's surface (≈ 725 ZJ) exceeds the current global primary energy

consumption by several orders of magnitude, underscoring the technical potential of solar energy to meet worldwide demand. The PV sector has evolved from a heavily subsidized technology to a self-sustaining and profitable industry, with global annual installations increasing from about 16 GW in 2010 to more than 150 GW in 2020, and continuous reductions observed in system costs. These trends position PVs as one of the fastest-growing and most scalable technologies for decarbonizing power systems.

Tropical countries, including Indonesia, are particularly well placed to benefit from PVs because of their high and relatively stable solar irradiance throughout the year. However, in many developing and emerging economies, large technical potential contrasts with relatively modest deployment, due to policy barriers, financing constraints, technical integration

challenges, and concerns about system reliability [3]. Improving the performance and robustness of PV systems under real operating conditions is therefore crucial to support wider adoption and to enhance their contribution to national energy and climate targets.

The output power of a PV is strongly influenced by irradiance, temperature, panel orientation, and shading, which makes the current–voltage and power–voltage characteristics highly nonlinear. To address this, Machine Learning (ML) utilization is required because ML can robustly handle the variables that strongly influence PV power generation, and achieve accurate forecasting results [4]. As part of Artificial Intelligence (AI), ML can operate effectively by analyzing data with complex trends and has been applied in various fields, including engineering [5].

The proposed hybrid Adaptive Neuro-Fuzzy Inference System (ANFIS) approach provides enhanced adaptability and optimization capacities for predicting the power generated by PV, offering particular benefits in handling the diverse and dynamic environmental conditions characteristic of Indonesia, specifically in Surabaya. In this study, an analysis and comparison of the ANFIS method, optimized using three metaheuristic methods, namely Genetic Algorithm (GA), Particle Swarm Optimization (PSO), and Cuckoo Search (CS), was carried out to derive the optimal forecast value for the power generated by PV. In addition, this study was developed as a continuation of [6]. The present study aims to provide valuable insights into the comparison between unoptimized and optimized ANFIS methods, which are beneficial for improving efficiency by forecasting the power generated by PV while supporting the transition to renewable energy resources.

Research has discussed PV output power forecasting by applying nonlinear-based methods. Authors in [7] utilized four prediction methods: Decision Tree, Random Forest (RF), Gradient Boosting, and Voting Regressor. Among these methods, RF achieved the highest accuracy (93.79 %). Authors in [8] utilized a hybrid prediction method, namely CNN-XGBoost, which achieved a Root Mean Square Error (RMSE) of 3.12 on the first day and 4.66 on the second day. Authors in [9] utilized a hybrid prediction method, namely the Long Short-Term Memory-Convolutional Neural Network (CNN-LSTM) transformer method. By utilizing the RMSProp optimizer, this hybrid method achieved a Mean Absolute Error (MAE) value of 0.58%. The application of the LSTM method was examined in [10], where two forecasting strategies were applied: recursive and Multiple-Input and Multiple-Output (MIMO). Each strategy was forecasted by the LSTM method. The mean value in the recursive strategy did not exceed 1.91 kW, and in the MIMO strategy, 1.22. The utilization of the Support Vector Regression (SVR) and Neural Network (NN) methods in combination with several metaheuristic methods was investigated in [11]. Two SVR and NN methods were employed, integrated with three optimization methods, namely Social Spider Optimization (SSO), PSO, and Cuckoo Search Optimization (CSO). The experiments conducted revealed that the PSO-Backpropagation Neural Network (PSO-BPNN) method outperformed other methods with an RMSE value of 3.251.

Research shows that various methods have been applied to solve this problem, ranging from basic, combinational, and hybrid methods. The forecasting results from each method achieved optimal performance based on the actual conditions at the test site. Therefore, this study applies a fuzzy-based method combined with adaptive neurons, namely ANFIS. This method was optimized using three different metaheuristic methods: GA, PSO, and CS.

II. RESEARCH METHOD

Figure 1 illustrates the research methodology employed in this study. Initially, the research problem was identified, specifically the comparison of the ANFIS method optimized by the GA, PSO, and CS methods in terms of their accuracy in forecasting the output power generated by PV. The data utilized in this study were derived from pilot test data conducted in Surabaya from May to September 2024. Subsequently, the data underwent further processing to identify trends, patterns, and tendencies that emerged during the trial period and were analyzed using statistical approaches. The data that had completed the statistical testing were moved to the forecasting modeling stage to create projections between the actual results and the 3 forecasts produced by these methods. The simulation results were compared based on their error values to determine which method demonstrated superior performance. In this work, the forecasting modeling process was conducted in three stages: the baseline stage involving the RF method, the implementation of ANFIS, and the optimized ANFIS.

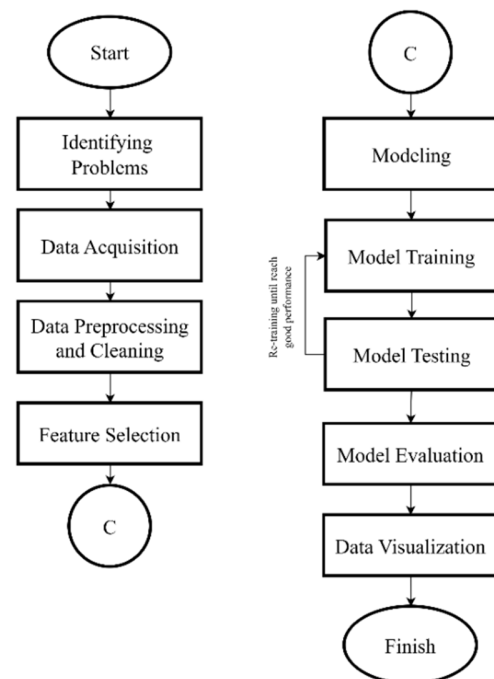


Fig. 1. Flowchart of the research method.

A. Data Acquisition

The comparison forecast of the PV power was based on ANFIS optimized by three metaheuristic methods, namely GA, PSO, and CS. The processed data were derived from field tests performed in Surabaya, specifically in the campus area. Testing had a time range limitation from May to September 2024. The dataset contained 1605 rows and 5 columns. The details of the dataset are presented in Table I.

TABLE I. DATASET

Trial	Temperature (°C)	Light intensity (lux)	Generated power (W)	Duration (h)
1	26.34	118.2	6.52	7
2	27.74	295	25.46	8
3	29.13	578	45.86	9

4	30.52	762	55.17	10
5	30.62	888	63.85	11
...
1605	29.73	704	53.75	16

Surabaya is the second largest city after Jakarta, the capital of Indonesia. This city is bordered by the two regencies of Sidoarjo and Gresik [12]. Furthermore, the city has an average temperature of 30 °C, with higher temperatures recorded during daytime.

B. Statistical Analysis

The process continued with the statistical analysis of the data. Table II provides the descriptive statistics and Figure 2 shows the distribution of all features.

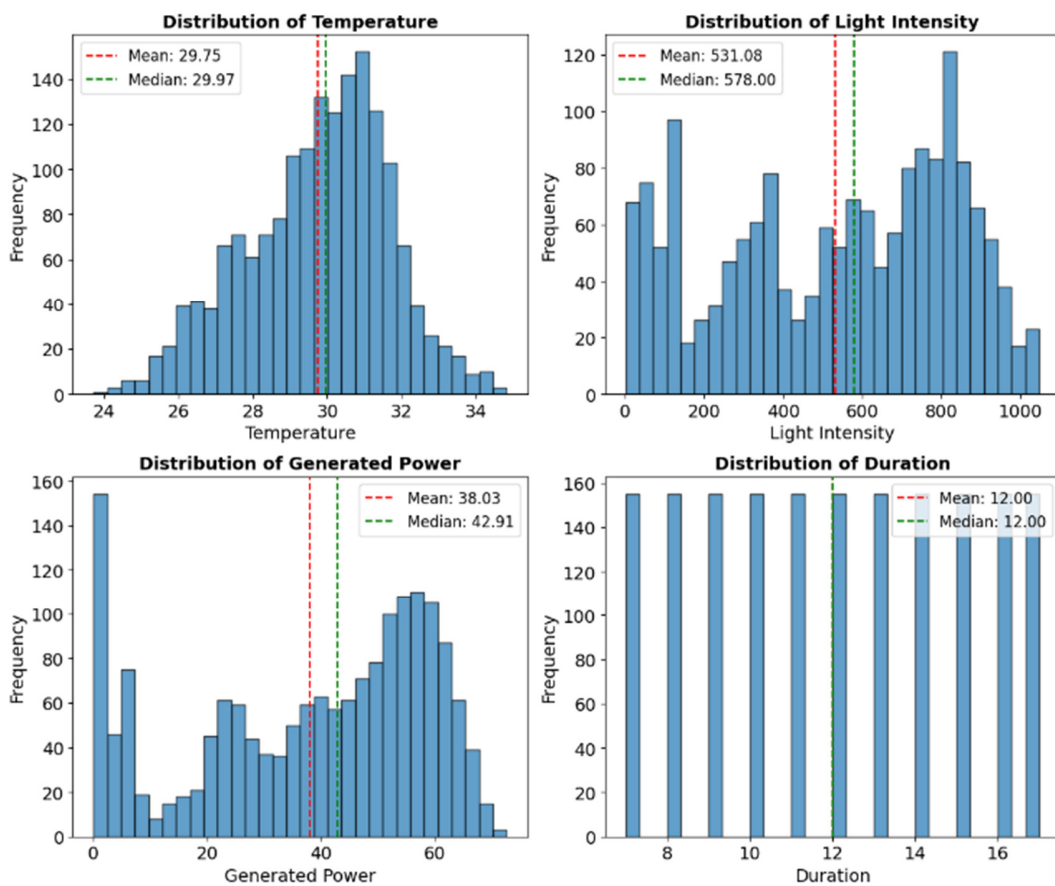


Fig. 2. Feature distribution plots.

TABLE II. DESCRIPTIVE STATISTICS

	Trial	Temperature (°C)	Light intensity (lux)	Generated power (W)	Duration (h)
Mean	853	29.74	531.08	38.03	12.00
Std	492.33	1.93	295.18	20.82	3.16
Min	1.0	23.71	1.00	0.00	7.00
Max	1705	34.84	1074.0	72.75	17.00

Figure 2 presents histograms of the data distribution across all features. None of the features are normally distributed.

Furthermore, the assumption that the data are not normally distributed is reinforced by the results of the normality test conducted by the Shapiro-Wilk test, the results of which are shown in Table III.

TABLE III. NORMALITY TEST

Temperature	Light Intensity
Temperature	stat = 0.9873, p-value = 0.0000
Light intensity	stat = 0.9403, p-value = 0.0000
Generated power	stat = 0.9164, p-value = 0.0000
Duration	stat = 0.9384, p-value = 0.0000

The results of the Autocorrelation and Partial Autocorrelation Functions (ACF and PACF) are illustrated in Figures 3 and 4. In Figure 3, it can be observed that many red nodes exceed the CI line (red), which means that the data are not stationary. The resulting pattern also corresponds to the conditions of the PV power measurements, namely, sharp increases and decreases due to environmental factors such as temperature and light intensity affecting the PV power. This is further explained in Figure 4, which demonstrates that a change occurred after lag 11. This change is indicated by the position of the green node on the CI line, implying that a weak partial correlation occurred.

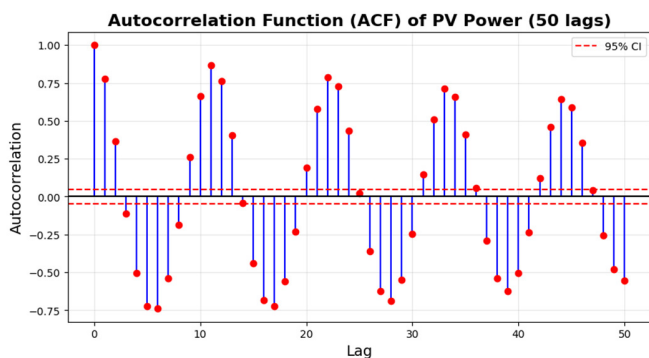


Fig. 3. The ACF plot.

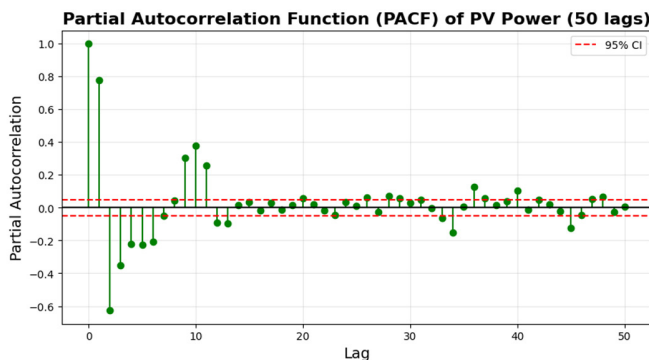


Fig. 4. The PACF plot.

Figure 5 reveals that the correlation between light intensity and generated power is 0.971, indicating a strong correlation between these two variables. Conversely, the correlation coefficient between temperature and the generated power is 0.489, suggesting a moderate correlation. The generated power features exhibit a strong negative correlation with duration. This observation implies that as the duration of the experiment increases, the generated power value decreases, potentially due to the diminishing intensity of sunlight as the day progresses towards evening. Based on the results of this correlation analysis, these three features can be considered input variables for forecasting the power generated by PV systems.

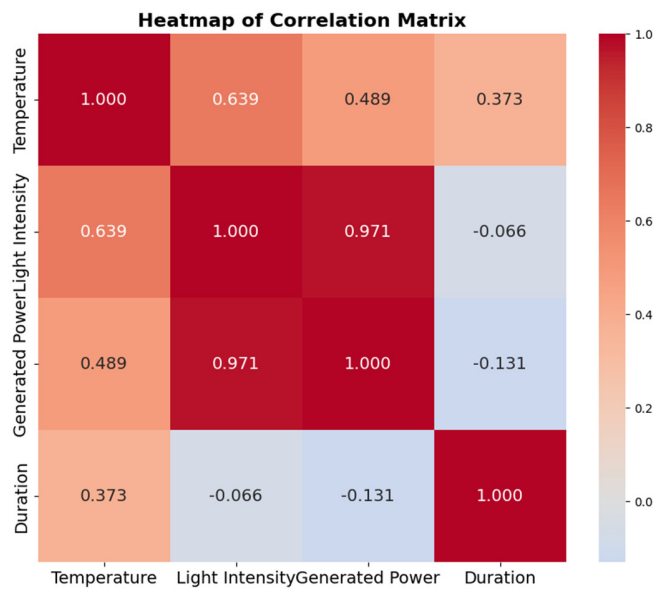


Fig. 5. Heatmap of the correlation test.

C. Adaptive Neuro Fuzzy Inference System

ANFIS is one of the supervised methods. This method combines the Takagi-Sugeno fuzzy inference system with an NN [13, 14]. Equations (1-6) demonstrate the steps for the ANFIS method:

$$\text{IF } x \text{ is } A \text{ and } y \text{ is } B, \text{ THEN } z = f(x, y) \tag{1}$$

Gaussian membership:

$$\mu(x) = \exp\left(-\left(\frac{x-c}{a}\right)^2\right) \tag{2}$$

Firing strength:

$$\mu_{Ai}(x) \cdot \mu_{Bi}(y) \quad i = 1, 2 \tag{3}$$

Normalized firing strength:

$$\bar{w}_i = \frac{w_i}{\sum_i w_i} \quad i = 1, 2 \tag{4}$$

Consequent:

$$\bar{w}_i f_i = \bar{w}_i (p_i x + q_i y + r_i) \quad i = 1, 2 \tag{5}$$

Summation of all input:

$$f = \frac{\sum w_i f_i}{\sum w_i} \tag{6}$$

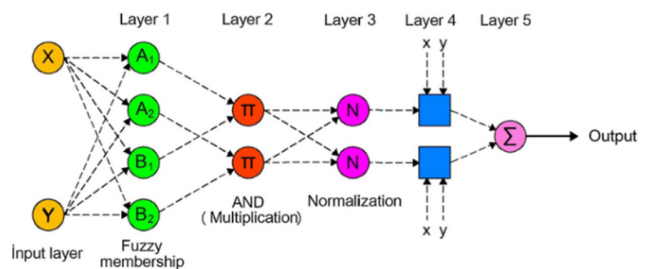


Fig. 6. ANFIS architecture.

The architecture of ANFIS is depicted in Figure 6, which shows that the ANFIS method employed in this study has five layers. In Layer 1, each input variable (temperature, light intensity, and duration) is mapped to a membership function using a Gaussian, as shown in (2). Layer 2 explains the fuzzy rules that represent "IF-THEN" rules and calculates the firing strength based on the "AND" operator, as demonstrated in (3). In Layer 3, the normalization process described by (4) is performed, which involves aggregating the firing strengths from the previous layer. In Layer 4, the consequent stage is described by (5) and the parameters learned by the NN are determined at this stage. Finally, Layer 5 involves summing all the outputs derived from the rules in the previous layers and converting the previous fuzzy results into crisp rules using the function (6).

D. Metaheuristic Methods and Evaluation Metric

The GA begins with a predefined population made up of numerous entities, each represented by a chromosome that indicates a potential solution for optimization. This approach uses crossover and mutation techniques to generate a range of solutions and employs selection methods to retain the most suitable individuals [15].

PSO is another metaheuristic method [16]. This method has two parameters: personal best and global best. The movement of particles to the near-global optimum is calculated by:

$$v_{id}(t + 1) = w_{ps0}(t) \cdot v_{id}(t) + c_1 \cdot r_{ps01} \cdot (p_{best} - x_{id}(t)) + c_2 \cdot r_{ps02} \cdot (g_{best} - x_{id}(t)) \tag{7}$$

$$i. x_{id}(t + 1) = x_{id}(t) + v_{id}(t + 1) \tag{8}$$

Finally, CS is an optimization method that depends on the Levy flight and is inspired by bird behavior observed when laying fertilized eggs [17]. The main equation for this method is:

$$x_i^{(t+1)} = x_i(t) + P_a \cdot S \cdot (x_i(t) - nest) \cdot randn(N) \tag{9}$$

To evaluate the performance of the optimized ANFIS method, the RMSE and R² score were employed using:

$$RMSE = \sqrt{\frac{1}{m} \sum_{i=1}^m (X_i - Y_i)^2} \tag{10}$$

$$R^2 = 1 - \frac{\sum_{i=1}^m (X_i - Y_i)^2}{\sum_{i=1}^m (\bar{Y} - Y_i)^2} \tag{11}$$

III. RESULTS AND DISCUSSION

A. Hyperparameters Tuning

The initial hyperparameters of the ANFIS method are listed in Table IV. These hyperparameters were also employed as a basis for the initial simulation before being optimized using metaheuristic methods. The details of the hyperparameters for the initial ANFIS method are described in Table IV. The details of the metaheuristic methods for the optimizer are described in Table V.

B. Simulation Results

In conducting the PV power forecasting process, trial initialization was performed using methods other than ANFIS.

In the present study, the RF method was applied. This method was chosen because of its ability to handle data that are nonlinear. In addition, using the RF method, the strength of the influence of the independent variables can be determined based on feature importance. Table VI shows the forecasting simulation results using the RF method, and Figure 7 depicts a plot that displays the importance of the features. For reference, the entire forecasting simulation process in this study was conducted using Python 3.10.

TABLE IV. THE INITIAL HYPERPARAMETERS OF THE BASIC ANFIS METHOD

Hyperparameter	Value
Input dimension	3
Membership function	Gaussian
Number of rules	27
Hidden rule layer 1	64
Hidden rule layer 2	32
Hidden rule layer 3	16
Consequent layer	1
Optimizer	Adam
Learning rate	0.001
Epoch	50
Early stopping	True

TABLE V. TUNING FOR THE OPTIMIZER METHODS

Method	Hyperparameter	Value
GA	Population size	6
	Generation	10
	Mutation rate	0.2
PSO	Particle size	8
	Iterations	15
	Inertia weight	0.7
	Cognitive	1.5
CS	Social	1.5
	Number of nests	15
	Abandon probability	0.25
	Levy flight scale	0.01
	Maximum iteration	20

TABLE VI. SIMULATION RESULTS OF THE RF

Simulation	Training data (%)	Testing data (%)	RMSE	R ² score
I	70	30	0.11	0.98
II	80	20	0.11	0.98
III	90	10	0.11	0.98

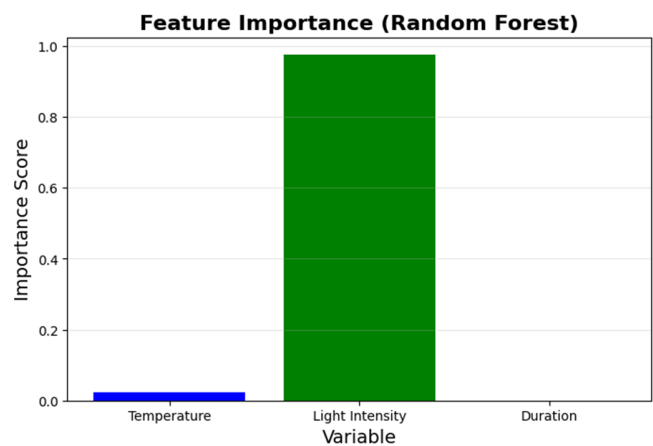


Fig. 7. Plot of feature importance.

Based on the results of the initial simulation tests using the RF method, the RMSE and R^2 values obtained were relatively constant at 0.11 and 0.98, respectively. The results were good, with the light intensity feature being quite dominant, exhibiting a value above 0.8. Meanwhile, the influence of the temperature and duration features was less than 0.2. Therefore, from these results, there is a possibility of further improvement using the ANFIS method.

In the next stage, simulation tests were conducted to improve the results by applying the ANFIS method without any optimization. The results are outlined in Table VII.

TABLE VII. THE SIMULATION RESULTS OF THE ANFIS

Simulation	Epoch	Training data (%)	Testing data (%)	RMSE	R^2 Score
I	50	70	30	0.67	0.99
II		80	20	0.62	0.99
III		90	10	0.49	0.99

As illustrated in Table VII, the simulation process was improved by optimizing it using metaheuristic methods. In the optimization process, several hyperparameters (including hidden layers 1 and 2) were focused on learning rate, dropout rate, and epoch. Furthermore, three different percentage ratios were applied in the split of the training and test data: 70:30, 80:20, and 90:10 (without randomization to prevent leakage). Figures 8-10 visualize the results of the ANFIS simulations optimized using the three metaheuristic methods.

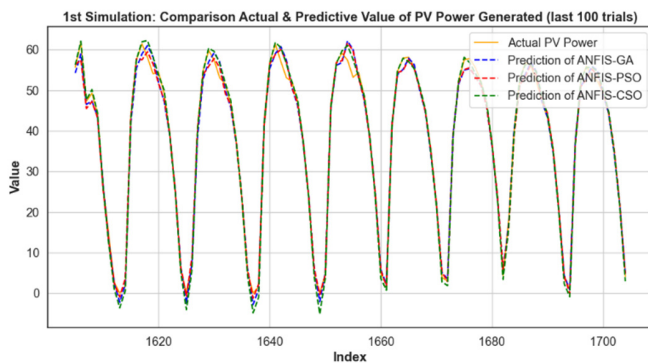


Fig. 8. The results of the first simulation (all ANFIS-optimized).

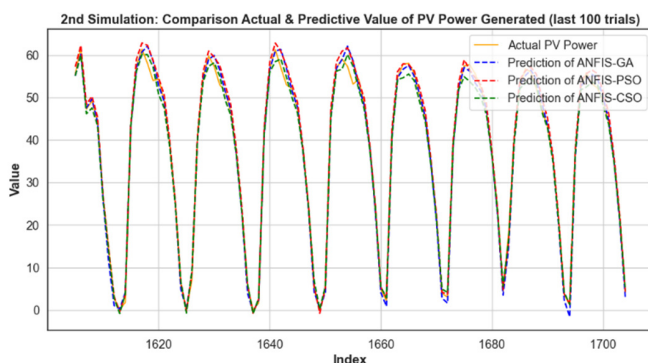


Fig. 9. The results of the second simulation (all ANFIS-optimized).

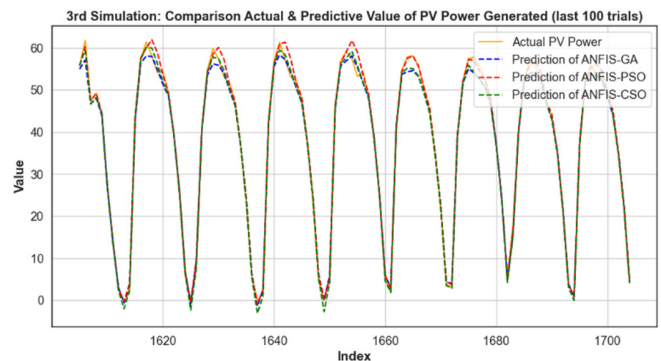


Fig. 10. The results of the third simulation (all ANFIS-optimized).

In Figures 8-10, it can be observed that the ANFIS method optimized by all the metaheuristic methods achieved satisfactory results by successfully approaching the actual values' line. Furthermore, as demonstrated in Figure 8, the forecast results obtained by the ANFIS-GA method come from a fitness value of 16.47. This configuration yielded an RMSE of 0.67 and an R^2 score of 0.99. For the ANFIS-PSO method with a global fitness value of 19, the results were an RMSE of 0.96 and an R^2 score of 0.99. For ANFIS-CS, with a global fitness score of 19.73, the results were an RMSE of 1.21 and an R^2 score of 0.99.

Figure 9 shows that in the second simulation, the forecast results obtained by the ANFIS-GA method were obtained from a fitness value of 22.58. This configuration yielded an RMSE of 1.14 and an R^2 score of 0.99. For the ANFIS-PSO method, with a global fitness value of 29, the results were an RMSE of 1.21 and an R^2 score of 0.99. For ANFIS-CS, with a global fitness score of 23.73, the results were an RMSE of 0.82 and an R^2 score of 0.99.

Finally, in Figure 10, it can be seen that in the third simulation, the forecast results obtained by the ANFIS-GA method originate from a fitness value of 23.21. This configuration yielded an RMSE of 1.13 and an R^2 score of 0.99. For the ANFIS-PSO method, with a global fitness value of 24.87, the results were an RMSE of 0.68 and an R^2 score of 0.99. For ANFIS-CS, with a global fitness score of 26.32, the results were an RMSE of 0.97 and an R^2 score of 0.99.

Based on the overall simulation results, the performance of the ANFIS method optimized using a metaheuristic method yielded satisfactory results. In addition, upon closer examination, it appears that the ANFIS method optimized using a meta-heuristic tends to be more stable in terms of performance, such that it does not result in significant discrepancies between simulation results, with a range of error values (RMSE) between 0.9 and 1.2. Some of the factors influencing this include data splitting and the hyperparameters generated by each optimization method. The differences obtained by the ANFIS method combined with metaheuristic methods during the simulation are illustrated in Figure 11.

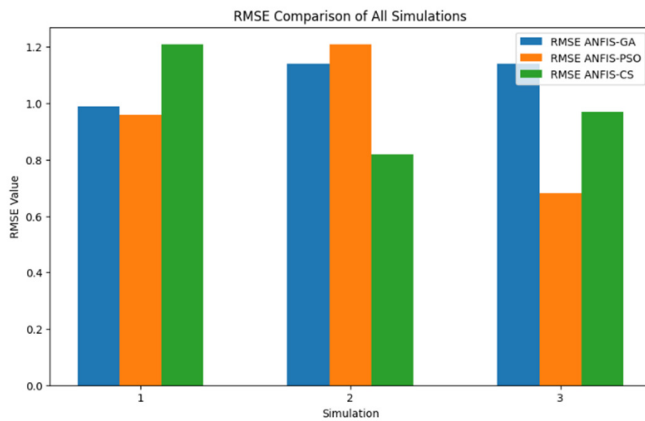


Fig. 11. RMSE comparison.

According to Figure 11, the RMSE values obtained by ANFIS combined with metaheuristic methods are dynamic. It can be observed that the RMSE values obtained by ANFIS-GA gradually increased. In contrast, for ANFIS-PSO, a significant decrease in the RMSE occurred in the third simulation, whereas for ANFIS-CS, it occurred in the second simulation. This phenomenon also indicates that each method has its own optimal point based on the resulting hyperparameters combined with the data split applied.

IV. CONCLUSIONS

The overall results of the simulations in this study were satisfactory and met the objectives of the study. The Adaptive Neuro-Fuzzy Inference System (ANFIS), combined with three metaheuristic optimization methods, produced satisfactory overall Root Mean Square Error (RMSE) values.

This study yielded several important findings. The ANFIS and optimized ANFIS methods resulted in an increase in the R^2 values, ranging from 0.98 to 0.99, compared to the previous results using the Random Forest (RF) method. A comparison of the RMSE values between the ANFIS and optimized ANFIS methods did not reveal any significant differences.

In this study, the metaheuristic method successfully demonstrated its consistency in maintaining forecasting error values, as evidenced by the resulting RMSE and R^2 scores. Of all the results from the simulations of the optimized ANFIS methods, the ANFIS-Particle Swarm Optimization (ANFIS-PSO) method yielded an RMSE value of 0.68, which was slightly better than the other two optimization methods.

Overall, the results of this study are expected to contribute to the advancement and development of the renewable energy transition in the future, especially in Surabaya. In future work, the proposed approach will be improved by adding dataset variants and applying more advanced forecasting technologies and case studies.

DECLARATION OF COMPETING INTERESTS

The authors declare that they have no known competing financial interests or personal relationships that could have influenced the work reported in this paper.

ACKNOWLEDGMENT

The authors would like to thank LPPM-Universitas Nahdlatul Ulama Surabaya for their support in providing the facility for this research. Additionally, gratitude is extended to the Centre of Research and Innovation Management of Universiti Teknikal Malaysia Melaka (UTeM) for sponsoring the publication fees under the Tabung Penerbitan CRIM UTeM.

DATA AVAILABILITY

All authors declare that the research data presented in this article are confidential.

AI USE AND DECLARATION OF GENERATIVE AI USE

All authors acknowledge that generative AI was utilized in the writing of this article; however, its utilization was limited to supporting research ideas and did not replace critical thinking or decision-making. All authors contributed to the writing and review of this article.

REFERENCES

- [1] W. S. Ebhota and T.-C. Jen, "Fossil Fuels Environmental Challenges and the Role of Solar Photovoltaic Technology Advances in Fast Tracking Hybrid Renewable Energy System," *International Journal of Precision Engineering and Manufacturing-Green Technology*, vol. 7, pp. 97–117, Jan. 2020, <https://doi.org/10.1007/s40684-019-00101-9>.
- [2] A. M. Mitrašinović, "Photovoltaics advancements for transition from renewable to clean energy," *Energy*, vol. 237, Dec. 2021, Art. no. 121510, <https://doi.org/10.1016/j.energy.2021.121510>.
- [3] S. M. Ashraf, M. S. B. Arif, M. Khouj, S. Md. Ayob, and M. I. Masud, "Python-Based Implementation of Metaheuristic MPPT Techniques: A Cost-Effective Framework for Solar Photovoltaic Systems in Developing Nations," *Energies*, vol. 18, no. 12, June 2025, Art. no. 3160, <https://doi.org/10.3390/en18123160>.
- [4] B. Zazoum, "Solar photovoltaic power prediction using different machine learning methods," *Energy Reports*, vol. 8, no. Supplement 1, pp. 19–25, Apr. 2022, <https://doi.org/10.1016/j.egyvr.2021.11.183>.
- [5] Y. Essam *et al.*, "Investigating photovoltaic solar power output forecasting using machine learning algorithms," *Engineering Applications of Computational Fluid Mechanics*, vol. 16, no. 1, pp. 2002–2034, Dec. 2022, <https://doi.org/10.1080/19942060.2022.2126528>.
- [6] R. A. Sinulingga *et al.*, "A Performance Comparison of the Extended Kalman Filter and the Unscented Kalman Filter for Photovoltaic Power Output Forecasting," *Engineering, Technology & Applied Science Research*, vol. 16, no. 1, pp. 30745–30750, Feb. 2026, <https://doi.org/10.48084/etasr.13866>.
- [7] V. Kolla, H. Mandula, A. V., and K. E., "Machine Learning-Driven Analysis and Prediction of Solar Power Generation for Enhanced Energy Management," in *2025 International Conference on Electronics and Renewable Systems (ICEARS)*, Feb. 2025, pp. 1640–1645, <https://doi.org/10.1109/ICEARS64219.2025.10940748>.
- [8] X. Zhang *et al.*, "Prediction of photovoltaic power generation based on a hybrid model," *Frontiers in Energy Research*, vol. 12, June 2024, Art. no. 1411461, <https://doi.org/10.3389/fenrg.2024.1411461>.
- [9] D. Salman, C. Direkoglu, M. Kusaf, and M. Fahrioglu, "Hybrid deep learning models for time series forecasting of solar power," *Neural Computing and Applications*, vol. 36, pp. 9095–9112, June 2024, <https://doi.org/10.1007/s00521-024-09558-5>.
- [10] R. Nelega *et al.*, "Prediction of Power Generation of a Photovoltaic Power Plant Based on Neural Networks," *IEEE Access*, vol. 11, pp. 20713–20724, 2023, <https://doi.org/10.1109/ACCESS.2023.3249484>.
- [11] M. Alrashidi and S. Rahman, "Short-term photovoltaic power production forecasting based on novel hybrid data-driven models," *Journal of Big*

- Data, vol. 10, Mar. 2023, Art. no. 26, <https://doi.org/10.1186/s40537-023-00706-7>.
- [12] J. Maulana and F. Bioresita, "Monitoring of Land Surface Temperature in Surabaya, Indonesia from 2013-2021 Using Landsat-8 Imagery and Google Earth Engine," *IOP Conference Series: Earth and Environmental Science*, vol. 1127, Jan. 2023, Art. no. 012027, <https://doi.org/10.1088/1755-1315/1127/1/012027>.
- [13] M. Ispir, M. H. Aksoy, and M. Kalyoncu, "Estimation of solar radiation and photovoltaic power potential of Türkiye using ANFIS," *Journal of King Saud University – Engineering Sciences*, vol. 37, Mar. 2025, Art. no. 2, <https://doi.org/10.1007/s44444-025-00002-0>.
- [14] D. Rahmalia *et al.*, "Comparison between Neural Network (NN) and Adaptive Neuro Fuzzy Inference System (ANFIS) on sunlight intensity prediction based on air temperature and humidity," *Journal of Physics: Conference Series*, vol. 1538, May 2020, Art. no. 012044, <https://doi.org/10.1088/1742-6596/1538/1/012044>.
- [15] W. M. N. Witharama, K. M. D. P. Bandara, M. I. Azeez, K. Bandara, V. Logeeshan, and C. Wanigasekara, "Advanced Genetic Algorithm for Optimal Microgrid Scheduling Considering Solar and Load Forecasting, Battery Degradation, and Demand Response Dynamics," *IEEE Access*, vol. 12, pp. 83269–83284, 2024, <https://doi.org/10.1109/ACCESS.2024.3412914>.
- [16] A. Kumar, M. Rizwan, and U. Nangia, "A Hybrid Intelligent Approach for Solar Photovoltaic Power Forecasting: Impact of Aerosol Data," *Arabian Journal for Science and Engineering*, vol. 45, no. 3, pp. 1715–1732, Mar. 2020, <https://doi.org/10.1007/s13369-019-04183-0>.
- [17] I. A. Hasan, M. Jawad, and B. Abdullah, "Characteristics Performance Prediction of PV Panel Using Cuckoo Search Algorithm," *IOP Conference Series: Materials Science and Engineering*, vol. 518, no. 3, May 2019, Art. no. 032033, <https://doi.org/10.1088/1757-899X/518/3/032033>.